

**Electronic Supplementary Information**

**TTE DNA-Cu NPs: Enhanced Fluorescence and Its Application  
in Target DNA Triggered Dual-Cycle Amplified Biosensor**

Guangfeng Wang<sup>a,b\*</sup>, Jing Wan<sup>a</sup>, Xiaojun Zhang<sup>a\*</sup>

<sup>a</sup> Anhui Key Laboratory of Chem-Biosensing, College of Chemistry and Materials Science, Center for Nanoscience and Nanotechnology, Anhui Normal University, Wuhu, 241000, P. R. China;

<sup>b</sup>State Key Laboratory of Chemo/Biosensing and Chemometrics, Hunan University, Changsha, 410082, PR China

**Contents**

- 1. The development and application of fluorescent DNA-Cu NPs**
- 2. Experimental Section**
- 3. Schematic Description of Scheme S1**
- 4. Feasibility of TTE DNA-Cu NPs Dual-cycle Amplified Biosensing Platform for Target DNA Detection.**
- 5. Optimization of the Detection Conditions.**
- 6. Scheme of the Control Experiment.**
- 7. Specificity and Practicality of the TTE DNA-Cu NPs Dual-cycle Amplification Biosensor.**
- 8. Table S3**

# 1. The development and application of fluorescent DNA-Cu NPs

**Table S1 The development and application of fluorescent DNA-Cu NPs**

DNA-template	Target detection	Fluorescence enhancement method	Ref.
ds DNA	---	---	[S1]
ds DNA	Adenosine-triphosphate	---	[S2]
ds DNA	Nucleotide	---	[S3]
ds DNA	Pb <sup>2+</sup>	---	[S4]
ds DNA	Sulfide anions	---	[S5]
ds DNA	Alkaline Phosphatase	---	[S6]
ds DNA	Nuclease enzyme	---	[S7]
ds DNA	Polynucleotidekinase	---	[S8]
ds DNA	---	---	[S9]
ds DNA	PDGF-BB	---	[S10]
ds DNA	DNA	polymerization-mediated	[S11]
ds DNA	MicroRNA	RCA	[S12]
ds DNA	DNA	HCR	[S13]
ds DNA	---	---	[S14]
ds DNA	Cancer cells andmicroRNAs	HCR	[S15]
ds DNA	Glucose	---	[S16]
ds DNA	L-histidine	---	[S17]
ds DNA	Dopamine	---	[S18]
ds DNA	Transcription Factors	---	[S19]
ds DNA	Dam MTase	---	[S20]
ds DNA	uracil-DNAglycosylase	---	[S21]
ss poly T	---	---	[S22]
ss poly T	Nuclease	---	[S23]
ss poly T	Copper ion	---	[S24]
ss poly T	Pb <sup>2+</sup> ion	---	[S25]
ss poly T	Terminal deoxynucleotidyltransferase	---	[S26]
ss poly T	Hydrogen peroxide	---	[S27]
ss poly T	Streptavidin	---	[S28]
ss poly T	Hg(II) ion	---	[S29]
ss poly T	N-acetylcysteine	---	[S30]
sspoly T	Glucose	---	[S31]
ss poly T	Trypsin	---	[S32]
ss poly T	Tumor DNA	---	[S33]
ss poly T	ATP	---	[S34]
ss poly T	DNA	---	[S35]
ds DNA- and ss poly T	NAD <sup>+</sup>	---	[S36]
ss poly T	Alkaline Phosphatase	---	[S37]

## 2. Experiment Section

**2.1 Chemicals and Reagents.** All oligonucleotide (listed in Table S2) with different sequences were synthesized and HPLC purified by Sangon Biotechnology Co. Ltd (Shanghai, China). Exonuclease III (exo III), 3-(N-Morpholino) propanesulfonic acid (MOPS, >99.0%), and sodium ascorbate (>99.0%) were commercially obtained from Sangon Biotechnology Co. Ltd (Shanghai, China). Other chemicals purchased from Sinopharm Chemical Reagent Co. Ltd. (Shanghai, China) were analytical grade and directly used without additional purification. The MOPS buffer (10 mM MOPS, 150 mMNaCl, pH 7.6) was used for the formation of fluorescent Cu NPs. MOPS buffer with various pH values were prepared by adjusting the ratio of the solution of 10 mM MOPS and 10 mMNaOH. All the stocks and buffer solutions were prepared by using ultrapure water (18.2 MΩ cm resistivity, PSDK2-10-C, Beijing, China)

To test the practicality of the proposed sensor, human serum samples were kindly obtained from the Yijishan Hospital (Wuhu, China). Before use, human serum samples were centrifuged at 10,000 rpm for 15 min, and then the supernatant was diluted with Tris-HCl for further use.

**2.2 Apparatus.** Ultraviolet-visible (UV-vis) absorbance measurements were performed on a UV-3010 spectrometer (Hitachi Ltd., Japan). Fluorescence spectra were determined by using a Hitachi F-4500 fluorescence spectrometer (Hitachi Ltd., Japan) controlled by FL Solution software. The optical path length of the quartz cuvette was 1.0 cm. Transmission electron micrograph (TEM) observations for the morphological measurements of Cu NPs were obtained with a Tecnai G220S-TWIN transmission electron microscope operating at an acceleration voltage of 200 kV. Absolute quantum yields (AQY) was measured using a FLS920 lifetime spectrometer (Edinburgh Analytical Instruments, England). A JASCO J-810 spectropolarimeter (Tokyo, Japan) was utilized to collect the circular dichroism (CD) spectra in the MOPS buffer. The optical chamber (0.1 cm path length) was deoxygenated with dry purified nitrogen (99.99%) before use and kept the nitrogen atmosphere during the experiments. The background of the buffer solution was subtracted from the CD data automatically. The pH values of MOPS buffer were measured with a glass electrode connected to a PHS-3C pH meter (Shanghai, China). Centrifugation was carried out by a HERMLEZ 36 HK apparatus (Wehingen, Germany). Fluorescence emission images were taken by a common digital camera (Shanghai, China).

**Table S2. The Name of Oligonucleotides (HP2, DNA 4 and 5 are released from HP1, HP3 and HP4, respectively.)**

Name	Sequences (from 5' to 3')
DNA 1	GAGTTGAGACCAT30TCAGAAGGCAAA
DNA 2	TTGCCTTCTGAT30TGGTCTCAACTC
HP1	ATGCATCATCTCTTCTCTTCCGGTCGAAATAGTGGGTAATATG CATAAAAAAATGCATCATCTCTTCTCTTCCGGTCGAAATAGTG GGTAATATGCATAGTCTGATAAGCTA
target DNA	TAGCTTATCAGA CTGATGTTGA
HP2	CATCTCTTCTCTTCCGGTCGAAATAGTGGGTAATATGCATAAA AAAATGCATCATCTCTTCTCTTCCGGTCGAAATAGTGGGTAAT
HP3	CACCACAAAGCGATCT30TATTGCTGATAAGCTAACCCACTATrAG GAAGAGACGTGGTG
HP4	CACCACTCAACATCAGTTATGTT30TAACGATCAACCCACTATrAG GAAGAGACGTGGTG
DNA 4	CACCACAAAGCGATCT30TATTGCTGATAAGCTAACCCACTAT
DNA 5	CACCACTCAACATCAGTTATGTT30TAACGATCAACCCACTAT
HP5	CGCGTGATCGTTAT30ACATACAATAT30GATCGCTTTCGCG
10 complementary base	GACCAT30TCAGA TCTGAT30TGGTC
20 complementary base	GTTGAGACCAT30TCAGAAGGCA TGCCTTCTGAT30TGGTCTCAAC
30 complementary base/(1) TTE DNA	GCAGAGTTGAGACCAT30TCAGAAGGCAAAAAA TTTTTTGCCTTCTGAT30TGGTCTCAACTCTGC
40 complementary base	CTCTCTTTTTGCCTTCTGAT30TGGTCTCAACTCTGCTCGAC GTCGAGCAGAGTTGAGACCAT30TCAGAAGGCAAAAAAGAGAG
one base mismatch	TAGCTTATCAGAGTGATGTTGA
Two base mismatch	TAGCTTATCCGAGTGATGTTGA
Three base mismatch	TAGCTTGTCCGAGTGATGTTGA
(2) TTE DNA	GCAGAGTTGAGACCACCCCT30CCCCCTCAGAAGGCAAAAAA TTTTTTGCCTTCTGACCCCT30CCCCCTGGTCTCAACTCTGC
(3) TTE DNA	GCAGAGTTGAGACCACCCCCCCCCCT30CCCCCCCCCTCAGAAG GCAAAAAA TTTTTTGCCTTCTGACCCCCCCCCCT30CCCCCCCCCTGGTCTCAA CTCTGC
(4) TTE DNA	GCAGAGTTGAGACCACCCCCCCCCCCCCCT30CCCCCCCCCCCC CCCTCAGAAGGCAAAAAA TTTTTTGCCTTCTGACCCCCCCCCCCCCCT30CCCCCCCCCCCC CTGGTCTCAACTCTGC

**2.3 Synthesis of TTE DNA-Cu NPs and 1-Cu NPs.** Prior to use, all the oligonucleotides stock solutions (100  $\mu\text{M}$ ) were prepared in 10 mM MOPS buffer and stored at 4  $^{\circ}\text{C}$  overnight. First, two complementary ssDNA (DNA 1 and 2) were mixed at the same molar ratios with the final concentration of 500 nM in 10 mM MOPS buffer into a 2 mL centrifuge tube labeled with “A”. The mixture was placed at room temperature for 20 min for future use. In order to carry out the control experiment, DNA 1 was added to another 2 mL centrifuge tube labeled with “B” at its final concentration of 1  $\mu\text{M}$  in 10 mM MOPS buffer. Then 16  $\mu\text{L}$  sodium ascorbate (100 mM) was added into the above solution, respectively. After incubation of 10 min at room temperature, 8  $\mu\text{L}$   $\text{CuSO}_4$  (10 mM) was introduced to the resulting solution in the centrifuge tube A and B and incubated for another 10 min under dark treatment to form TTE DNA-Cu NPs and 1-Cu NPs. The final volumes of the two tubes were both 270  $\mu\text{L}$ . Finally, the resulted solutions were characterized by fluorescence spectrophotometer and the excimer fluorescence was recorded.

**2.4 TEM Characterization of TTE DNA-Cu NPs and 1-Cu NPs.** Samples of were prepared by spin coating 10  $\mu\text{L}$  of the as-prepared TTE DNA-Cu NPs or 1-Cu NPs onto carbon-coated copper grid substrates, which were then dried naturally overnight and measured by Tecnai G220S-TWIN.

**2.5 Fluorescence Measurement.** The excitation wavelength was 340 nm and the emission spectra were recorded from 480 to 670 nm. The slit widths for excitation and emission were set at 5 and 10 nm. All fluorescence measurements were carried out at Hitachi F-4500 fluorescence spectrophotometer with excitation at 340 nm and emission at 615 nm. When the samples were excited at 340 nm, the emission was scanned from 480 to 670 nm in steps of 0.5 nm; the excitation and emission slits of the spectrophotometer were set at 5.0 nm and 10.0 nm; the scanning speed was 1200 nm  $\text{min}^{-1}$ .

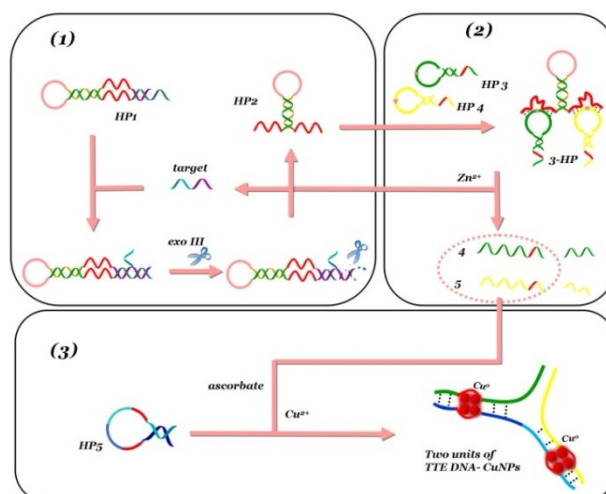
**2.6 Gel Electrophoresis.** In the gel electrophoresis assay, each prepared sample (8  $\mu\text{L}$ ) was put on 5% agarose gels to separate the related substances. The electrophoresis was carried in 0.5  $\times$ TBE buffer (pH 7.9) at 120 V constant voltage for 1 h. After EB staining, the gels were scanned using the Omega 16ic Gel imaging system (ULTRA-LUM, USA).

**2.7 Fabrication of TTE DNA-Cu NPs Dual-cycle Amplification Biosensor and the Control Experiment.** The working solution was obtained by diluting the stock solution with 10 mM MOPS buffer. The hairpin-like HP1, HP3, HP4 and HP5 solution were heated to 90  $^{\circ}\text{C}$  for 10 min to remove aggregates, and then cooled slowly to room temperature at a constant rate over the course of 2 h to form the stem-loop structure, respectively before use.

First, 1  $\mu\text{M}$  hairpin-like HP1 and target DNA were incubated for 30 min at room temperature in MOPS buffer solution. Second, the reaction solution was incubated with 12 U exo III at 37  $^{\circ}\text{C}$  for 35 min. After the digestion by exo III, the reaction was terminated through heating at 85  $^{\circ}\text{C}$  for 15 min to inactivate exo III. Third, 1 nM  $\text{Zn}^{2+}$  was added to the above mixture to initiate the cleavage reaction at rA for 40 min. Finally, 16  $\mu\text{L}$  sodium ascorbate (100 mM) and 8  $\mu\text{L}$   $\text{CuSO}_4$  (10 mM) were added to prepare fluorescent TTE DNA-Cu NPs. The final volume was 270  $\mu\text{L}$ .

Control experiment with conventional polyT DNA-Cu NPs was carried out. In this strategy, 2  $\mu\text{M}$  hairpin-like HP1 treated with 1  $\mu\text{M}$  target DNA were incubated for 30 min at room temperature in MOPS buffer solution. Then 12 U *exo III* was added at 37  $^{\circ}\text{C}$  for 35 min. After the digestion by *exo III*, heating at 85  $^{\circ}\text{C}$  for 15 min to inactivate *exo III*, 2 nM  $\text{Zn}^{2+}$  was added for 40 min. The following process is the same as the TTE DNA based dual cycle strategy.

### 3. Schematic Description of Scheme S1



**Scheme S1** Schematic illustration of biosensing protocol based on TTE DNA-Cu NPs with autocatalytic dual-cycle amplification for target DNA detection

As shown in Scheme S1, the hairpin DNA (HP1) which has a blue part of the tailored nucleic acid structure was designed containing the recognition site sequences of the target DNA and the red part corresponding to the nucleic acid sequence of  $\text{Zn}^{2+}$  dependent 8-17 DNAzyme.<sup>23</sup> The strategy contained three process: (1) In the presence of the target DNA, it can hybridize with HP1 and the product would be digested by *exo III* which can specifically recognize the sequence of a double-stranded part of HP1 with a blunt end at the 3' terminus. Then, the target DNA and hairpin 2 (HP2) would be released. The liberated target DNA becomes available to trigger the successive reaction cycle leading to the generation of a large amount of HP2. (2) Meanwhile, two other hairpin DNA (HP3 and HP4) with polyT sequences at the tail of the stems are rationally designed to recognize the region of the generated DNAzyme in HP2 and participate in the second cycle. When the  $\text{Zn}^{2+}$  is added, the cleavage of  $\text{Zn}^{2+}$  at the rA position of HP3 and HP4, 4 and 5 is liberated. (3) Subsequently, when the hairpin DNA (HP5) is introduced into the above system, 4 and 5 can hybridize with and unfold HP5, forming a "Y"-shaped DNA containing two TTE DNA structure units to produce a strong fluorescent signal. In contrast, without the target DNA, the HP1 can't be digested by the *exo III* unable to form the DNAzyme and no reactions can be triggered. The HP3 and HP4 remain stable, in spite of the presence of the *exo III* and  $\text{Zn}^{2+}$ . Therefore, the strategy through the synergistic combination of TTE DNA-Cu NPs with the dual-cycle is hopeful to offer a feasible way for the target DNA detection.

#### 4. Feasibility of the TTE DNA-Cu NPs Dual-cycle Amplified Biosensing Platform for Target DNA Detection.

To verify the feasibility of the proposed assay strategy, fluorescent signal obtained upon analyzing the target DNA and those obtained in a series of control experiments are depicted in Fig. S1. As curve b of Fig. S1A shows, in the absence of the target DNA, the fluorescent signals are low, because the HP1 could not be unfolded to initiate HP2 to form  $Zn^{2+}$ -dependent-DNAzyme, resulting in DNA 4 and 5 of the downstream cycle unable to be released into solution for further formation of “Y” shaped TTE DNA-Cu NPs. However, due to the polyT sequences at the tail of the stems of HP3, HP4 and the loop of HP5 provided conjugated sites to form the fluorescent Cu NPs, the weak fluorescent signal still existed. Upon the addition of the target DNA, a significantly increased fluorescent signal can be observed indicating the unfolded HP1 triggered the occurrence of the subsequent exo III assisted cycling cleavage process producing HP2 to participate in the  $Zn^{2+}$  cleaved cycle to bring large amounts of “Y” shaped TTE DNA-Cu NPs as detectable indicator causing an obvious fluorescent signal enhancement (curve a of Fig. S2A). In addition, it was found that the absence of exo III would also cause a decrease in the fluorescent signal (curve b of Fig. S2B). It was deduced that without exo III, HP2 could not be formed and the following reaction would not carry out, which is just like that in the absence of the target DNA. Meanwhile, the weak fluorescent signal in curve b of Fig. S2C told us without HP3+HP4, the HP2 would not be cleaved by  $Zn^{2+}$  unable to release 4, 5. But because HP5 contained polyT sequences in the loop, there was a weak fluorescence of Cu NPs. Due to the  $Zn^{2+}$  cleavage cycle could not happen without the addition of  $Zn^{2+}$ , the fluorescence also has a little decrease as curve b in Fig. S2D shows, but the weak fluorescence may be from the fluorescent Cu NPs on poly T in the tail of the unfolded HP3 and HP4 and the loop part of HP5. An even lower fluorescence of Cu NPs was observed without the addition of HP5 (curve b of Fig. S2E), indicating the successful release of 4 and 5 could not form an effective DNA scaffold as “Y” shaped TTE DNA for highly fluorescent Cu NPs. The results proved exo III,  $Zn^{2+}$ , HP3+HP4 or HP5 is essential for the dual-cycle amplification system operated to form “Y” shaped TTE structure. Therefore, the aforementioned results clearly demonstrated the designed TTE DNA-Cu NPs based fluorescent strategy could pave a new way to detect target DNA and the fluorescent signal amplification is indeed resulting from the “Y” shaped TTE DNA-Cu NPs.

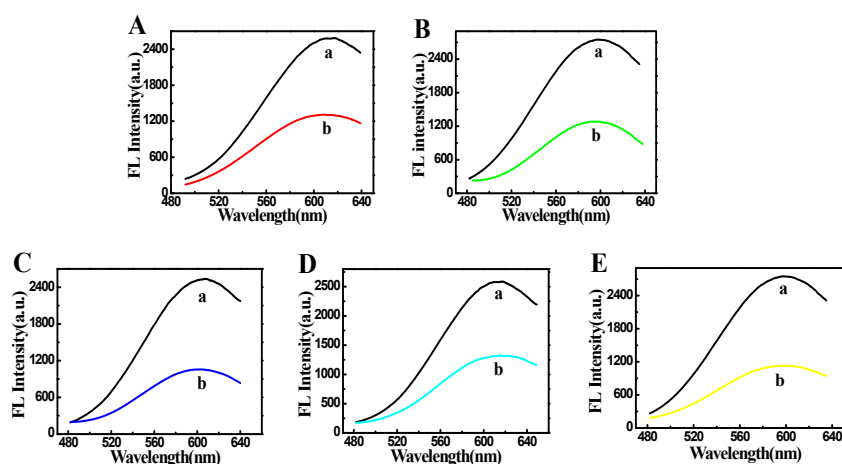


Fig. S1 Response of the solution with (a) and without (b) target DNA (A), exo III (B), HP3+HP4 (C),  $Zn^{2+}$  (D) or HP5 (E) through using fluorescent monitoring in the dual-cycle amplification strategy, respectively.

### 5. Optimization of the Detection Conditions.

We next thought to test the utility of this strategy for the detection of target DNA. In order to do so, some factors, which are in correlation with the performance of fluorescence measurements, have been investigated in detail. Since the reaction time and the concentration of exo III have significant influence on the amplification reaction, the systems with different exo III concentrations and reaction time were investigated, respectively. Fig. S2A shows that the fluorescent intensity was enhanced when the concentration of the exo III was increased from 0 to 12 U. It arrived at a maximum of 12 U, when the concentration of the probe DNA was over  $1 \mu M$ , the fluorescent response tends to be stable. Therefore, 12 U was selected as the optimal concentration for TTE DNA-Cu NPs biosensing. The value of F increases with the digestion time and the maximum value of F is obtained when the digestion time of exo III is 35 min (Fig. S2B).

$Zn^{2+}$  is important for  $Zn^{2+}$ -dependent DNAzyme-assisted amplification, which is key for the detection performance. The concentration of cofactor  $Zn^{2+}$  and the catalytic time of the DNAzyme were also optimized, respectively. As shown in Fig. S2C, the fluorescence intensity increases rapidly with the increasing  $Zn^{2+}$  concentration at first and then decreases when the  $Zn^{2+}$  concentration is higher than 1.0 nM. The highest fluorescence intensity is obtained when the final concentration of  $Zn^{2+}$  is 1.0 nM. The result is possibly attributed to the fact that the concentration of  $Zn^{2+}$  is higher than 1.0 nM would affect the activity of exo III, causing reduction of the TTE structure finally. Furthermore, the catalytic time of  $Zn^{2+}$  and DNAzyme approaches to a plateau within 40 min (Fig. S2D).

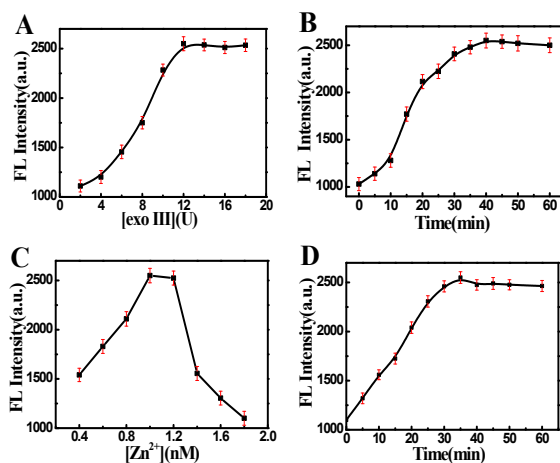
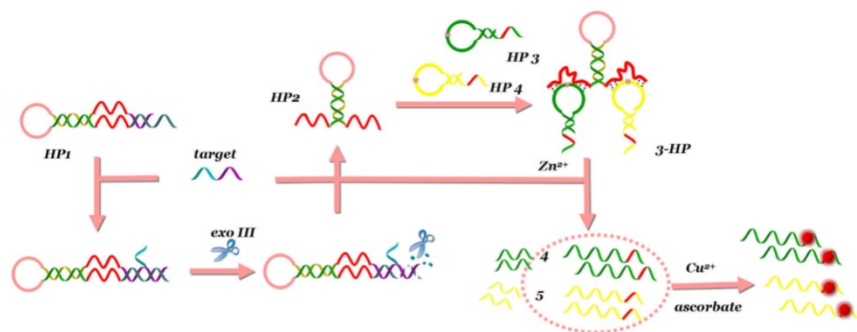


Fig. S2 (A) Variance of the value of F with exo III concentration from 2 to 18 U; (B) Digestion reaction time from 0 to 60 min in the exo III-aided autocatalytic target recycling system; (C) Variance of the value of F with the concentration of  $Zn^{2+}$  (0.4, 0.6, 0.8, 1.0, 1.2, 1.6 and 1.8 nM); (D) Catalytic time of  $Zn^{2+}$  and DNAzyme from 0 to 60 min.



## 6. Scheme of the Control Experiment.



**Scheme S2** Schematic of the control experiment.

Control experiment without HP5 in the system towards series concentrations of target DNA was investigated. The schematic design of the control is shown in Fig. 3C. As can be seen, since there is no HP5 in the solution, the Cu NPs would grow on polyT sequences of free released DNA 4 and 5 templates.

### 7. Specificity and Practicality of the TTE DNA-Cu NPs Dual-cycle Amplification Biosensor.

The sequence discrimination of the autocatalytic dual-cycle amplification was investigated (Fig. S3). The specific response of the biosensing protocol to target DNA is evaluated by examining the fluorescent signal of the Cu NPs solution in the presence of various DNA (“one-base-mismatched, two-base-mismatched, three-base-mismatched” with target DNA in Table S2) under the same conditions. The result shows that only the addition of target DNA can induce a prominent increase in the fluorescent emission of the TTE DNA templated Cu NPs biosensor, demonstrating that our sensing system has a high specificity for target DNA. In addition, the practicality of the proposed strategy was applied to detect target DNA by analyzing different dilution ratios (1:50, 1:100) of human serum samples under the same detection procedure as that described in the aforementioned experiment. As can be seen from Table S3 samples, all the results obtained indicated a satisfactory application of the strategy.

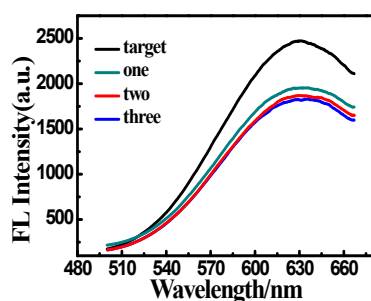


Fig. S3 Fluorescent intensity of complementary DNA (target), single-base mismatched DNA (one), two-bases mismatched DNA (two) and three-bases mismatched DNA (three) in TTE DNA-Cu NPs dual-cycle amplification biosensor.

**8. Table S3****Table S3 Determination of target DNA added in the real sample**

Dilution	Added (mol/L)	Founded (n=3) mol/L	Recovery (%)	R. S. D (%)
1:50	$10^{-11}$	$9.75 \times 10^{-10}$	97.5	4.16
	$10^{-9}$	$1.02 \times 10^{-9}$	102	5.92
	$10^{-7}$	$9.8 \times 10^{-6}$	98	5.19
1:100	$10^{-11}$	$9.92 \times 10^{-10}$	99.2	4.95
	$10^{-9}$	$1.02 \times 10^{-14}$	102	5.53
	$10^{-7}$	$9.85 \times 10^{-6}$	98.5	6.17

## Reference:

- [S1] A. Rotaru, S. Dutta, E. Jentsch, et al. *Angew. Chem. Int. Ed.*, 2010, **49**, 5665–5667.
- [S2] Z. Zhou, Y. Du, S. Dong, *Anal. Chem.* 2011, **83**, 5122–5127.
- [S3] X. Jia, J. Li, L. Han, et al. *ACS nano*, 2012, **6**, 3311–3317.
- [S4] J. Chen, J. Liu, Z. Fang, et al. *Chem. Commun.*, 2012, **48**, 1057–1059.
- [S5] J. Liu, J. Chen, Z. Fang, et al. *Analyst*, 2012, **137**, 5502–5505.
- [S6] L. Zhang, J. Zhao, M. Duan, et al. *Anal. Chem.*, 2013, **85**, 3797–3801
- [S7] R. Hu, Y. R. Liu, R. M. Kong, et al. *Biosens. Bioelectron.*, 2013, **42**, 31–35.
- [S8] L. Zhang, J. Zhao, H. Zhang, et al. *Biosens. Bioelectron.*, 2013, **44**, 6–9.
- [S9] T. Qing, Z. Qing, *RSC Advances*, 2014, **4**, 61092–61095.
- [S10] X. H. Yang, S. Sun, P. Liu, et al. *Chinese Chemical Letters*, 2014, **25**, 9–14.
- [S11] Z. Qing, T. Qing, Z. Mao, et al., *Chem. Commun.*, 2014, **50**, 12746.
- [S12] F. Xu, H. Shi, X. He, et al. *Anal. Chem.*, 2014, **86**, 6976–6982.
- [S13] C. Song, X. Yang, K. Wang, et al. *Anal. Chim. Acta*, 2014, **827**, 74–79.
- [S14] Q. Song, Y. Shi, D. He, et al. *Chem. Eur. J.*, 2015, **21**, 2417–2422
- [S15] Y. Zhang, Z. Chen, Y. Tao, et al. *Chem. Commun.*, 2015, **51**, 11496–11499
- [S16] H. B. Wang, H. D. Zhang, Y. Chen, et al. *RSC Adv.*, 2015, **5**, 77906
- [S17] H. B. Wang, H. D. Zhang, Y. Chen, et al. *New J. Chem.*, 2015, **39**, 8896–8900
- [S18] H. B. Wang, H. D. Zhang, Y. Chen, et al. *Sens. & Actuat. B*, 2015, **220**, 146–153
- [S19] L. Sha, X. Zhang, G. Wang, *Biosens. Bioelectron.*, 2016, **82**, 85–92.
- [S20] Q. Q. Lai, M. D. Liu, C. C. Gu, et al. *Analyst*, 2016, **141**, 1383–1389.
- [S21] M. Cao, Y. Jin, B. Li, *Anal. Methods*, 2016, **8**, 4319–4323.
- [S22] Z. Qing, X. He, D. He, et al. *Angew. Chem. Int. Ed.* 2013, **52**, 9719–9722.
- [S23] Z. Qing, X. He, T. Qing, et al. *Anal. Chem.*, 2013, **85**, 12138–12143
- [S24] Z. Qing, Z. Mao, T. Qing, et al. *Anal. Chem.* 2014, **86**, 11263–11268.
- [S25] L. J. Ou, X. Y. Li, H. W. Liu, et al. *Anal. Sci.*, 2014, **30**, 723–727.
- [S26] T. Ye, C. Li, C. Su, et al., *Chem. Commun.*, 2015, **51**, 8644–8647.
- [S27] Z. Mao, Z. Qing, T. Qing, et al. *Anal. Chem.*, 2015, **87**, 7454–7460.
- [S28] H. B. Wang, H. D. Zhang, Y. Chen, et al., *Biosens. Bioelectron.*, 2015, **74**, 581–586.
- [S29] H. B. Wang, Y. Chen, Y. Li, et al. *RSC Adv.*, 2015, **5**, 94099–94104
- [S30] H. B. Wang, H. D. Zhang, Y. Chen, et al. *Anal. Methods*, 2015, **7**, 6372
- [S31] H. B. Wang, H. D. Zhang, Y. Chen, et al. *RSC Adv.*, 2015, **5**, 77906–77912.
- [S32] L. J. Ou, X. Y. Li, L. J. Li, et al. *Analyst*, 2015, **140**, 1871–1875.
- [S33] Q. Zhou, J. Zheng, Z. Qing, et al. *Anal. Chem.*, 2016, **88**, 4759–4765.
- [S34] J. Chen, X. Ji, P. Tinnefeld, et al. *ACS Appl. Mater. Interfaces*, 2016, **8**, 1786–1794.
- [S35] W. Hu, Y. Ning, J. Kong, et al. *Analyst*, 2015, **140**, 5678–5684.
- [S36] Y. Wang, H. Cui, Z. Cao, et al. *Talanta*, 2016, **154**, 574–580.
- [S37] J. Y. Li, L. Si, J. C. Bao, Z. Y. Wang, Z. H. Dai, *Anal. Chem.*, 2017, **89**, 3681–3686.